Transactions of the **13th International Conference on Structural Mechanics in Reactor Technology** (SMiRT 13), Escola de Engenharia - Universidade Federal do Rio Grande do Sul, Porto Alegre, Brazil, August 13-18, 1995

Comparison between VISA-II and OCA-P for probabilistic fracture mechanics analysis focusing on analysis method

Hirano, M.[1], Watanabe, N.[1], Tatewaki, I.[2], Akiba, H.[2]
1) Japan Atomic Energy Research Institute, Ibaraki-ken, Japan
2) Allied Engineering Corporation, Tokyo, Japan

ABSTRACT: Probabilistic fracture mechanics (PFM) analyses have been widely applied to evaluate the failure probabilities of reactor pressure vessels of pressurized water reactors subjected to pressurized thermal shock. In the present study, a comparison between the VISA-II and OCA-P codes for PFM analyses was performed to clarify the differences in the numerical processes. For this purpose, the benchmark problems proposed by the U.S. Nuclear regulatory Commission and the Electric Power Research Institute were applied. This paper discusses the algorithm to evaluate the deviations from the means of RT_{NDT} and fracture toughness, and the numerical treatment of initial flaw depth as the major differences in these codes.

1. INTRODUCTION

The probabilistic fracture mechanics (PFM) technique has already been involved in the regulatory practices in the U.S.A. It is stated in the Regulatory Guide 1.154 of the Nuclear Regulatory Commission (NRC) that "if the plant-specific pressurized thermal shock (PTS) analyses predict that the PTS-related, through wall crack penetration mean frequency will remain less than $5x10^{-6}$ per reactor year for the requested period of continued operation, such operation would be acceptable to the staff"(U.S.NRC 1987). It is also stated that "the calculations should be performed with a PFM code such as OCA-P(Cheverton et al. 1984) or VISA-II(Simonen et al. 1986)". These codes apply the Monte Carlo simulation to evaluate the flaw initiation probability and vessel failure probability.

In the present study, the numerical methods in OCA-P and VISA-II were compared as a preparatory step to upgrade the physical models to be used for mainly aging research. In-depth understanding of numerics is essential to assess the effect of improvement of physical models. Along the same line, in order to supply proper basis for comparisons between not only physical models but also numerical methods, the U.S. NRC and the Electric Power Research Institute (EPRI) have proposed and performed benchmark exercise for PFM in 1991(Bishop 1993) which consists of more than twenty cases from simple ones to rather complicated ones. In the present study, two very simple cases were selected for the present purpose and calculated with both OCA-P and VISA-II. As a result, significant differences appeared. This paper discusses the algorithm to evaluate the deviations from the means of RT_{NDT} and fracture toughness, and the numerical treatment of initial flaw depth as the major sources of the differences.

2. BENCHMARK CASES APPLIED IN PRESENT STUDY

The benchmark cases applied in the present study are those named Case B1 and Case B2, whose major specifications are summarized in Table 1. The reactor coolant temperature transient is specified by a simple exponential curve with a constant pressure. The flaws are assumed to be circumferential and the cladding at inside surface of the vessel wall is neglected. The differences between Cases B1 and B2 are only the deviations from the mean values of such as ΔRT_{NDT} and neutron fluence, which are assumed to follow a normal distribution with each respective standard deviation σ. As shown in Table 1, certain values are specified for the standard deviations in Case B1, while all these are specified to be zero in Case B2.

3. MAJOR DIFFERENCES IN NUMERICAL METHODS

Simplified flow charts in VISA-II and OCA-P on the calculation of a single flaw are shown in Fig.1(a). The initial flaw depth is determined by generating a random number following a flaw depth distribution. The major differences in the numerics for probabilistic analysis in these codes are summarized as follows:

(1) Treatment of Initial Flaw Depth and Grid Spacing

In VISA-II, the initial flaw depth distribution can be specified by inputs as a function of flaw depth (discrete points) and the initial flaw depth is treated continuously by interpolating this initial flaw depth distribution. After an initiation of flaw growth ($K_I > K_{Ic}$), the other grid, which is basically equal spacing with a fixed grid width Δz, is used for flaw growth calculation, and the flaw growth length is calculated in the unit of Δz (see "(A)" in Fig.1(a)). In OCA-P, the Marshall distribution is installed for the initial flaw depth distribution and the depth is treated discretely based on the grid whose spacing is fixed to be a geometric progression. The flaw growth length is calculated on this grid without interpolation. This difference is discussed related to Case B2.

(2) Algorithm to Evaluate Deviations from Mean values

In VISA-II, not only the means of K_{Ia} and RT_{NDT} but also their deviations, δK_{Ia} and δRT_{NDT}, respectively, are revaluated during the flaw growth calculation (see "(A)" in Fig.1(a)). Further, the mean value of K_{Ic} and its deviation, δK_{Ic}, are revaluated after the arrest (see "(B)" in Fig.1(a)). In OCA-P, basically the same algorithm is applied but δRT_{NDT} is not revaluated (see also "(C)" in Fig.1(a)). Hereafter, we call the algorithms mentioned above applied in VISA-II and OCA-P the VISA model and OCA model, respectively. This difference is discussed related to Case B1.

4. CALCULATED RESULTS AND DISCUSSIONS

4.1 Case B1

Figure 2 shows the comparison between the results with OCA-P and VISA-II, for Cases B1. A remarkable difference appears. In order to clarify the difference, the OCA model is implemented into VISA-II and the VISA model is implemented into OCA-P. The results are compared in Fig.3. A good agreement was obtained. It was confirmed that the effect of difference in grid mentioned in (1) in Sec.3 was small in this case. Therefore, the major source of the difference is whether or not δRT_{NDT} is revaluated in the flaw growth calculation. Figure 4 shows the results of the sensitivity calculation on the standard deviation of initial RT_{NDT}, σ_{RTNDT0}, setting both σ_{KIa} and σ_{KIc} equal to zero. It is shown that δRT_{NDT} has a large effect to reduce the vessel failure probability in the VISA model.

(1)Defect in OCA and VISA Models

In order to clarify the reason why δRT_{NDT} has such a large effect on the vessel failure probability, a model which we call the Constant model is introduced. In this model, as shown in Fig.1(b), the deviations δRT_{NDT}, δK_{Ia} and δK_{Ic} are evaluated only once per one flaw. Figure 5 shows the numbers of arrested non-failure flaws as a function of the flaw growth length in the unit of Δz for the VISA, OCA and Constant models. As shown in this figure, the flaws tend to be arrested during a small number of iterations, most in the VISA model and then in the OCA model. As already mentioned, δK_{Ia} (and δRT_{NDT} in VISA model) is repeatedly revaluated within the iteration loop to search the flaw depth at arrest in the OCA and VISA models. Then, if δK_{Ia} is calculated, by chance, to be a large negative value as a result of generating a random number, the flaw is arrested. This means that the chance to be arrested increases if the number of times to generate random numbers for δK_{Ia} or δRT_{NDT} increases, and this fact well explains the results shown in Fig.5. Similar situation can appear if Δz is reduced, since the number of times increases. As expected, as shown in Fig.6, the vessel failure probability decreases as Δz is reduced, and convergence is not achieved, though it basically should not depend on Δz. This is considered to be a defect. It makes sense that neither δRT_{NDT} nor δK_{Ia} should be revaluated within the iteration loop to search the flaw depth at arrest, because this iteration is a numerical process and does not simulate the physical flaw growth process.

If we follow the assumption that the deviations δK_{Ia} and δRT_{NDT} are dependent on the location in the vessel wall, they should be revaluated every time when a flaw grows. But, it is enough to revaluate them just once every time after the flaw initiation or re-initiation takes place, as shown in Fig.1(c). It is because the values of δK_{Ia} and δRT_{NDT} revaluated just once can be understood as the predicted ones at the depth at arrest, though it is unknown at that moment. Then the physical meaning becomes clear, and we call this model the Realistic model.

(2)Comparison between Various Algorithms to Evaluate Deviations

Another possibility considered in the present study is an algorithm where neither δK_{Ia} nor δRT_{NDT} is revaluated at all after initiation in the Realistic model. This model apparently gives conservative results in comparison with the Realistic model. Then we call it the Conservative model. The only difference between the Constant model stated in (1) and the Conservative model is that δK_{Ic} is not revaluated after arrest in the Constant model.

Figure 7 shows the comparison between five models mentioned above. The VISA model gives remarkably lower vessel failure probability than the Realistic model as expected. In the OCA model, the deviation δRT_{NDT} is not revaluated at all and this could explain the reason why it gives higher probability than the Realistic model. The Constant model and Conservative model give higher probabilities than the Realistic model, as expected. The reason why the Conservative model gives lower probability than the Constant model is that the chance of flaw re-initiation after arrest is reduced, because the deviation δK_{Ic} is revaluated after arrest. This effect is not considered to be numerical but physical.

4.2 Case B2

Figures 8 and 9 show the results from sensitivity calculations with VISA-II and OCA-P, respectively, on σ_{RTNDT}, where all the other standard deviations such as σ_{KIa}, σ_{KIc} and σ_f are assumed to be zero. Therefore, the cases with σ_{RTNDT}=0 in the figures

correspond to Case B2. As shown in Fig.9, OCA-P gives discontinuous behavior. Although similar tendency also appears in VISA-II, it is not remarkable.

This discontinuous behavior in OCA-P is originated by the numerical treatment of initial flaw depth. As described in (1) in Sec.3, it is treated discretely in OCA-P. In Case B2, since all the standard deviations are zero, a threshold value f_i of fluence exists corresponding to a flaw depth z_i and all the flaws with depths z_k, $k>i$ are initiated to grow. Therefore, the flaw initiation probability $P_I(f)$ can be written as

$$P_I(f) = P_{Ii} = \sum_{k=i}^{n} N_k \quad \left(\sum_{k=1}^{n} N_k\right) : \text{constant} \quad \text{for } f_i \le f < f_{i-1} \quad (i = 1, n) \tag{1}$$

where N_k is the number of initial flaws with depth z_k and n is the number of grid cells. It is shown that $P_I(f)$ is a stair-shaped function with respect to f. In VISA-II, the initial flaw depth is treated continuously by interpolating the initial flaw depth distribution and therefore, this discontinuity basically does not exist. When the deviation of, for example, fluence is taken into consideration in Eq. (1), the flaw initiation probability can be written as follows:

$$P_I(f) = \sum_{k=1}^{n} P_{Ik} \cdot \int_{f_{k+1}-f}^{f_k - f} \phi(f, f')df' \tag{2}$$

where $\phi(f_m, \delta f)$ is the probability density function of deviation δf from the mean f_m of fluence. Equation (2) shows that $P_I(f)$ becomes a continuous function of f when taking into account the deviation, because the integral terms in Eq.(2) are continuous function of f.

As summary, the initial flaw depth should be treated continuously by interpolating the depth distribution in order to avoid unphysical results when all the standard deviations are small.

5. CONCLUDING REMARKS

The numerical methods of VISA-II and OCA-P were compared by applying the EPRI/NRC benchmark exercise. The major concluding remarks derived are summarized as follows:

(1) It is confirmed that the major source of the difference between OCA-P and VISA-II is the algorithm to evaluate the deviations from the mean value of RT_{NDT}.

(2) It was shown that the vessel failure probability decreases when the grid width Δz is reduced and no convergence is achieved in OCA-P and VISA-II. The reason is that the deviation of K_{Ia} (and RT_{NDT} in VISA-II) is repeatedly revaluated within the numerical iteration loop to search the flaw depth at arrest.

(3) In order to avoid the difficulty mentioned above, a slight modification was done following an assumption that the deviations depend on flaw depth. By comparing various models including a model with the modification, the effect of the algorithm to evaluate the deviations was quantified.

(4) The initial flaw depth is treated continuously in VISA-II but discretely in OCA-P. It is shown that the method in OCA-P gives seriously unphysical results when all the standard deviations of random variables are small.

REFERENCES

U.S.NRC 1987. Regulatory Guide 1.154, January.

Cheverton, R.D. and Ball, D.G. 1984 . OCA-P, A Deterministic and Probabilistic Fracture Mechanics Code for Application to Pressure Vessels, NUREG/CR-3618.
Simonen, F.A, et al. 1986. VISA-II - A Computer Code for Predicting the Probability of Reactor Pressure Vessel Failure, NUREG/CR-4486, PNL-5775.
Bishop, B.A. 1993. Benchmarking of Probabilistic Fracture Mechanics Analysis of Reactor Vessels Subjected to Pressurized Thermal Shock (PTS) Loading, EPRI Research Project 2975-5, Final Report, March (Draft for Review).

Table 1 Major Specifications for Cases B1 and B2

Reactor Vessel Geometry		
Wall thickness	9 inch (Cladding thickness=0)	
Vessel Inside radius	90 inch	
Coolant Conditions		
Temperature	$T_i + (T_t - T_i)\exp(-0.15t)$ °F T_i = 150, T_t = 550, t : time in min	
Pressure	1000 psig	
Heat transfer coeff.	320 Btu/(hr ft^2· F)	
Flaw Depth Distribution	Original OCTAVIA distribution	
Flaw Orientation	Circumferential (360° extent)	
Random Variables(Normal distribution)	mean	standard deviation
Initial RT $_{NDT}$	20° F	17° F
Cu:Copper content	0.3 w%	0.025 w%
Ni:Nikckel content	0.75 w%	0.0
Fluence	0.5 to 3x10^{19} n/cm^2	30% of mean
ΔRT_{NDT}	RG 1.99, Rev.2 *1)	0.0
K_{Ia} , K_{Ic}	given by equations*2)	10% of mean
Fluence Attenuation	exp(-0.024a), a:depth into wall in inch	
Upper Shelf Toughness	200 ksi·in$^{0.5}$	
Failure Criteria	Flaw depth reaches 100% of wall thickness Remaining regament exceeds flow stress of 80 ksi	

*1) $\Delta RT_{NDT} = CF \cdot f^{(0.28 - 0.10\log_{10} f)}$
f:neutron fluence divided by 10^{19}
CF = 217.25 for 0.3w%Cu and 0.75w%Ni

*2) $K_{Ic} = 36.2 + 49.4\exp(0.0104\delta T)$ for δT <-50° F
$= 55.1 + 28.0\exp(0.0214\delta T)$ for δT >-50° F
$K_{Ia} = 19.9 + 43.9\exp(0.00993\delta T)$ for δT <+50° F
$= 70.1 + 6.50\exp(0.01960\delta T)$ for δT >+50° F
$\delta T = T - RT_{NDT}$
T:temperature at crack tip (F)

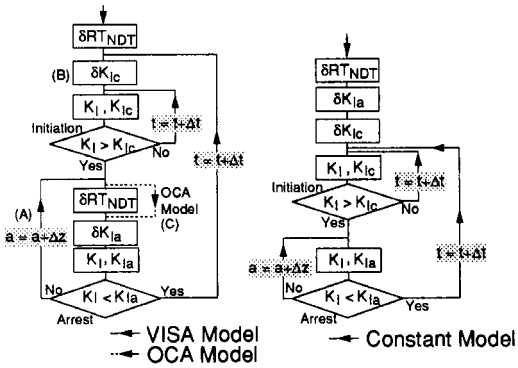

(a) VISA and OCA models (b) Constant model

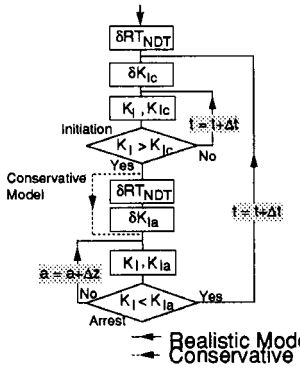

(c) Realistic and Conservative models

Fig. 1 Simplified Flow Chart for One Flaw

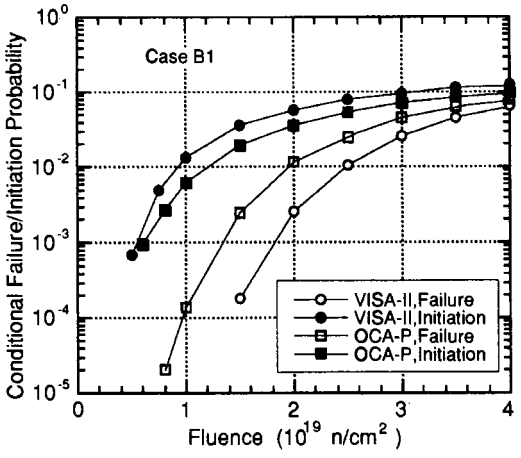

Fig. 2 Comparison between OCA-P and VISA-II (Case B1)

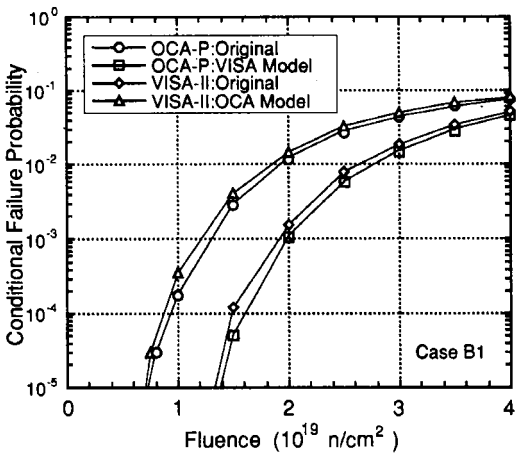

Fig. 3 Comparison between OCA-P with VISA Model and VISA-II with OCA Model (Case B1)

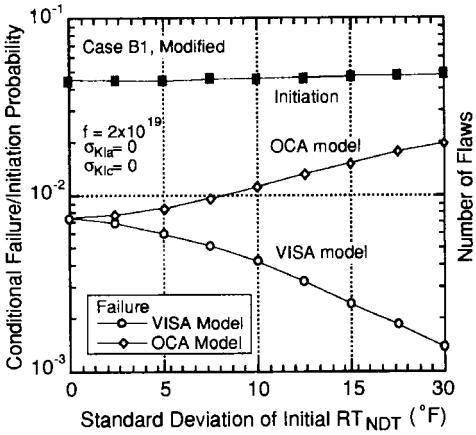

Fig.4 Sensitivity Calculations on σ_{RTNDT0} in VISA and OCA models (Calculations done with VISA-II)

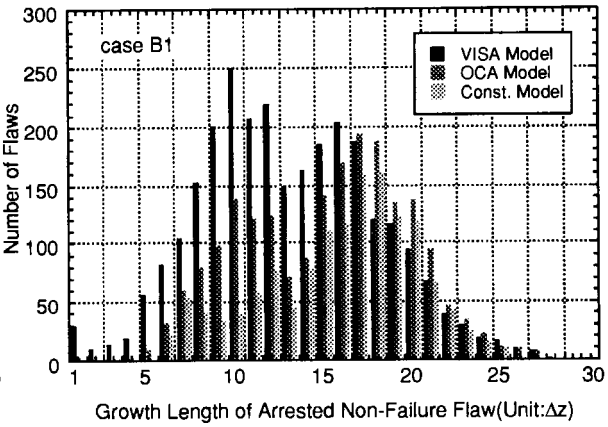

Fig.5 Calculated Numbers of Arrested Non-Failure Flaws as a function of Flaw Growth Length in Various Models for case B1 (Calculations done with VISA-II)

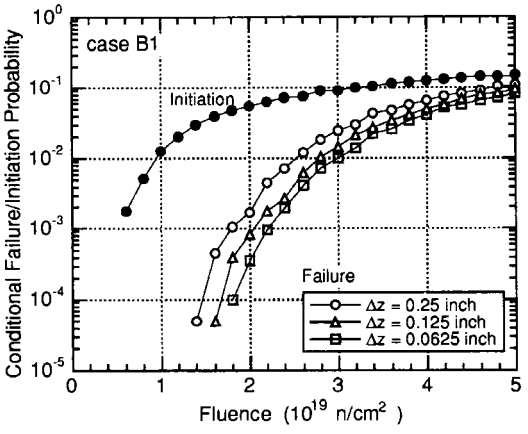

Fig.6 Sensitivity Calculation on Grid Width with VISA-II (Case B1)

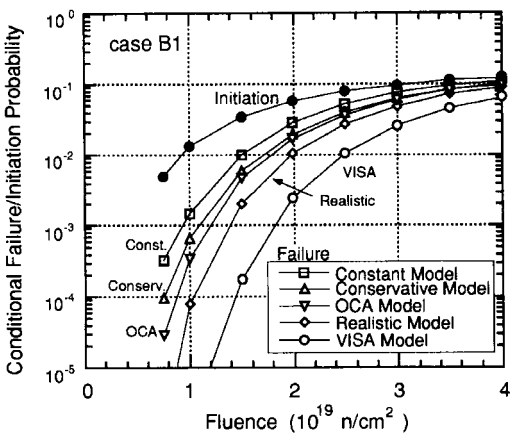

Fig.7 Comparison between Various Algorithms to Evaluate Deviations (Calculations done with VISA-II)

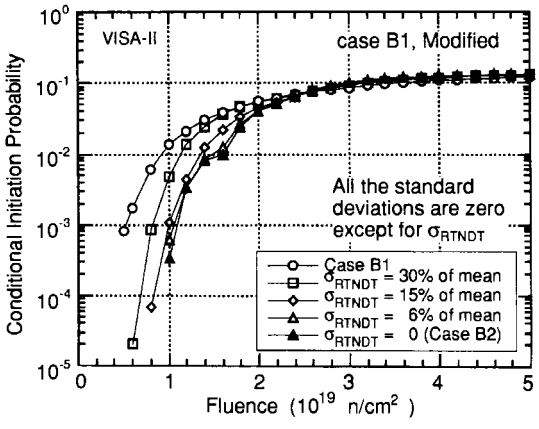

Fig.8 Sensitivity Calculation on σ_{RTNDT} in VISA -II

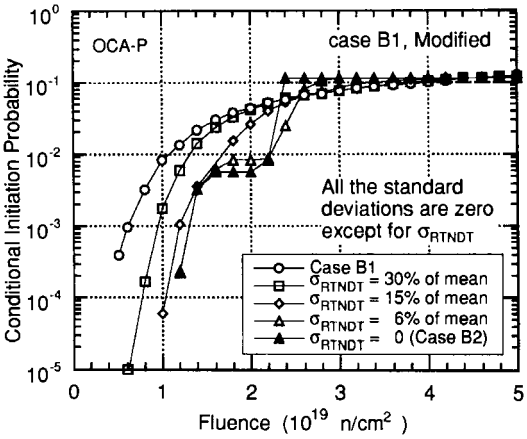

Fig.9 Sensitivity Calculation on σ_{RTNDT} in OCA-P